Supporting Information

A Highly Active Perovskite Anode with in Situ Exsolved Nanoalloy Catalyst for Direct Carbon Solid Oxide Fuel Cells

Minjian Ma, Xiaoxia Yang, Rongzheng Ren, Chunming Xu, Jinshuo Qiao, Wang Sun, Kening Sun and Zhenhua Wang*

Beijing Key Laboratory for Chemical Power Source and Green Catalysis, School of

Chemistry and Chemical Engineering, Beijing Institute of Technology, Beijing,
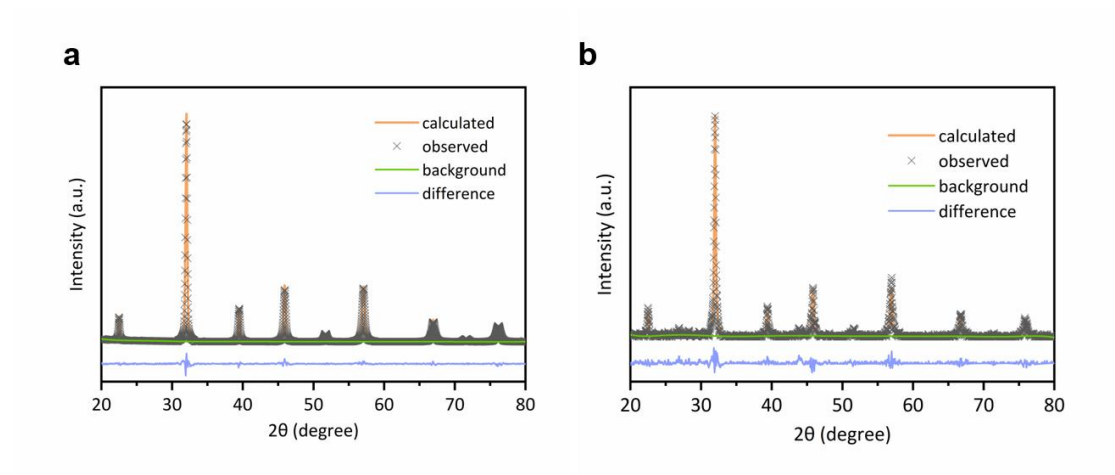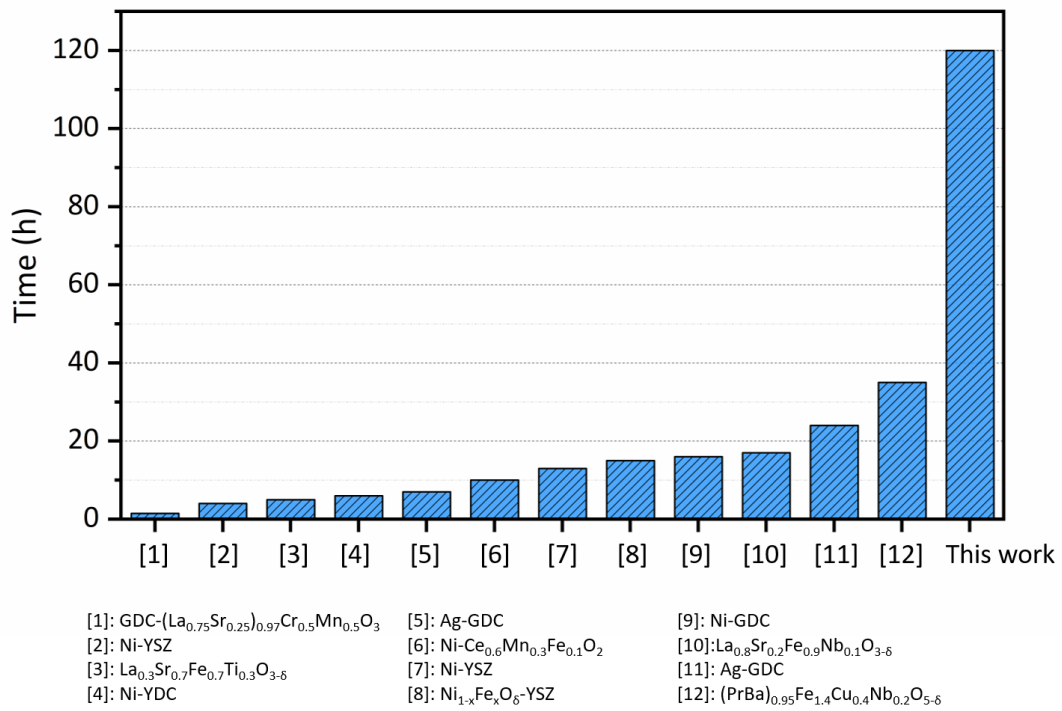
100081,

People's Republic of China

AUTHOR INFORMATION

Corresponding Author

*Email: wangzh@bit.edu.cn (Zhenhua Wang).

1. Supporting figures

Figure S1. XRD refinement data of PBFNN (a) and FeNi$_3$@PBFNN (b) based on the tetragonal lattice geometry of the space group P4/mmm.

Figure S2. Comparison of the stability of the DCSOFC technology with different anodes, stability refers to the stable time before performance degradation of the cells. The anode materials used in each research are listed under the figure and the corresponding references are listed in section 3 (Supporting reference).
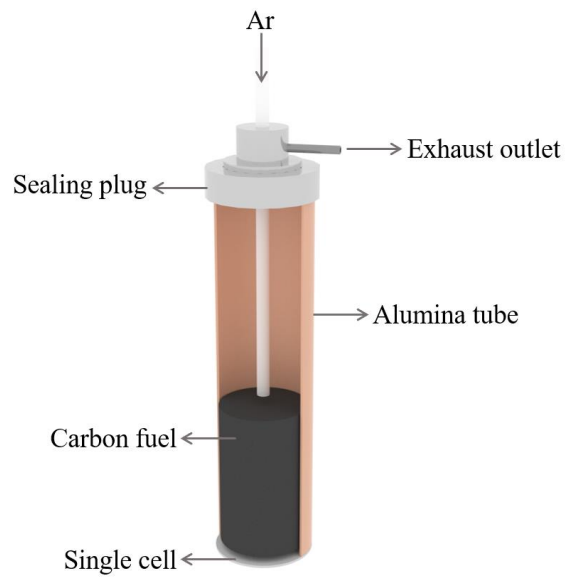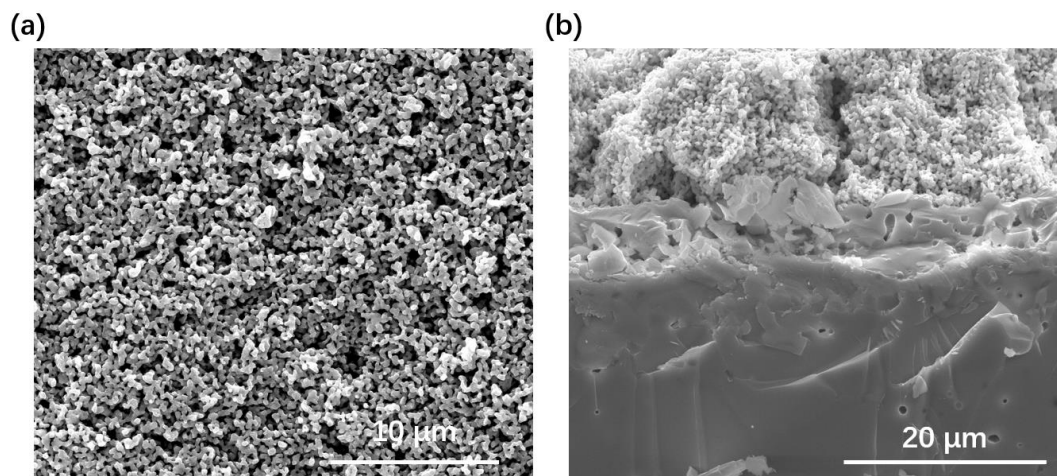
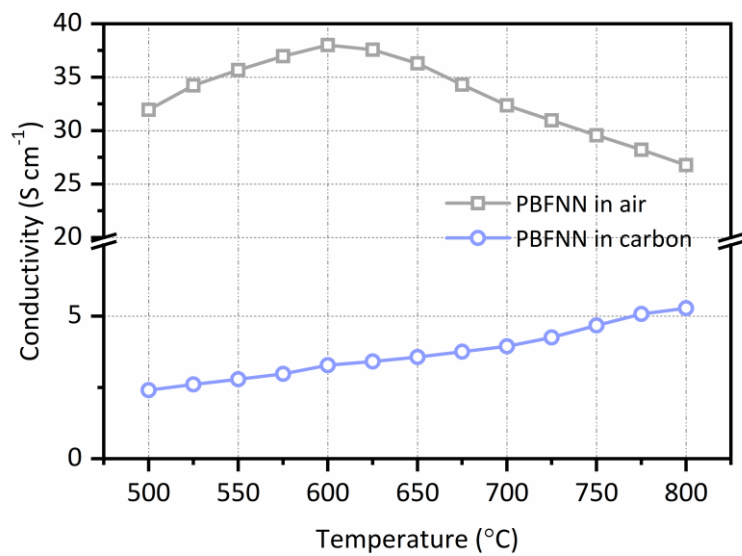**Figure S3**. Schematic view of the test device used in this work.
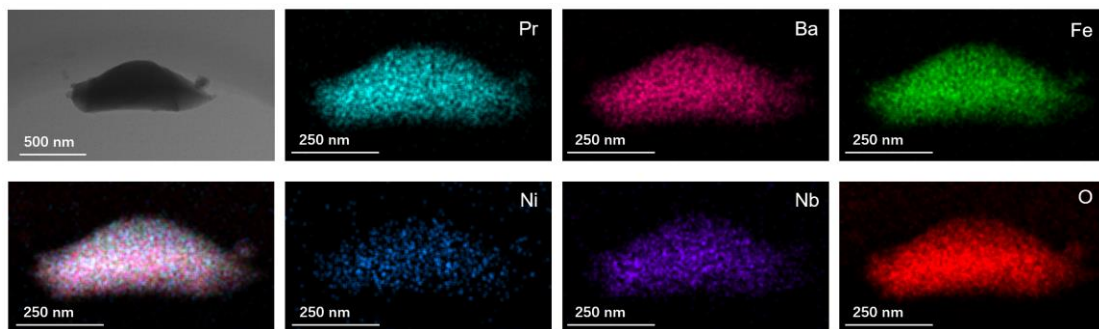
Figure S4. STEM images and the EDS mappings of as-prepared PBFNN powders in HAADF-STEM mode.
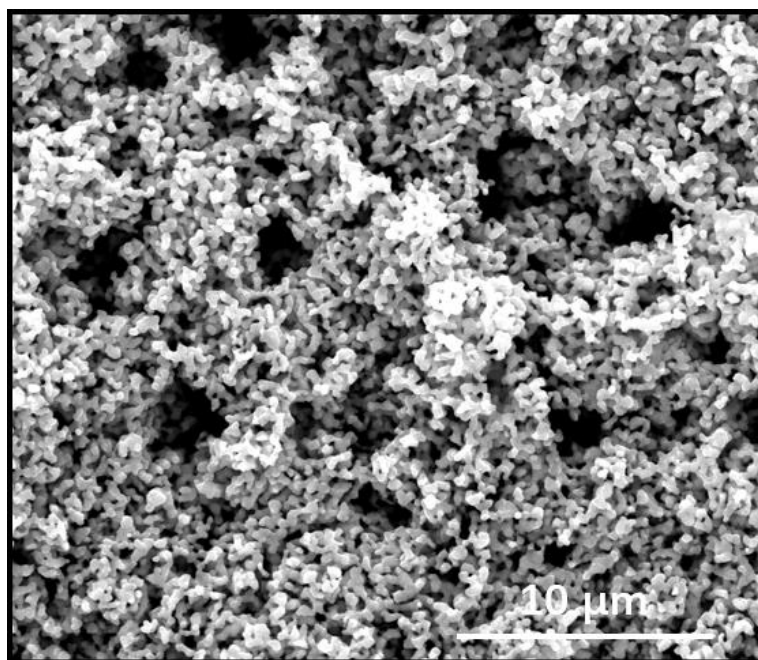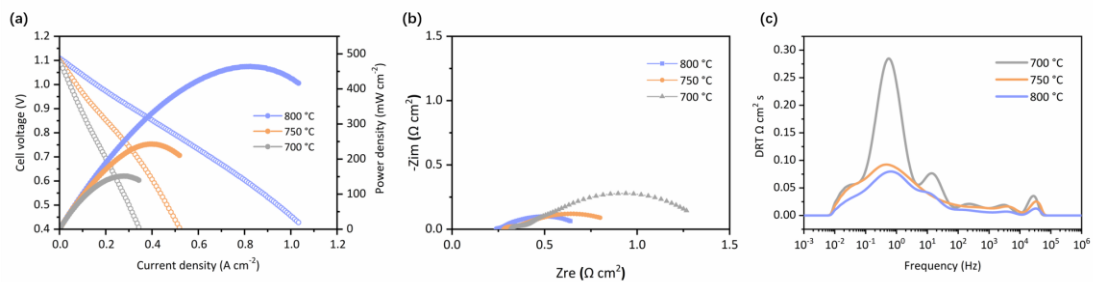
Figure S5. SEM image of as-prepared PBFNN powder.

Figure S6. Microstructure of the as-prepared anode (a) and the cross-sectional image of the single cell (b).

Figure S7. Temperature-dependent conductivity of PBFNN in air and in activated carbon.

Figure S8. Electrochemical performance analysis of the HDCFC with PBFNN as the anode: (a) The I-V-P curves of the cell; (b) The corresponding electrochemical impedance spectra measured under OCV conditions; (c) The DRT plots of the single cell.
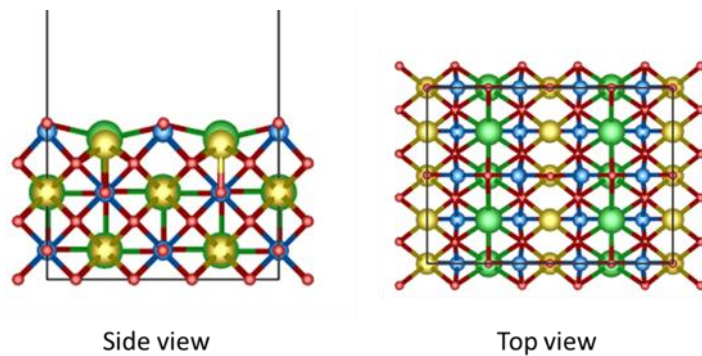
Side view   Top view

Figure S9. Side view and top view of the used slab model of $Pr_{0.5}Ba_{0.5}FeO_3$.
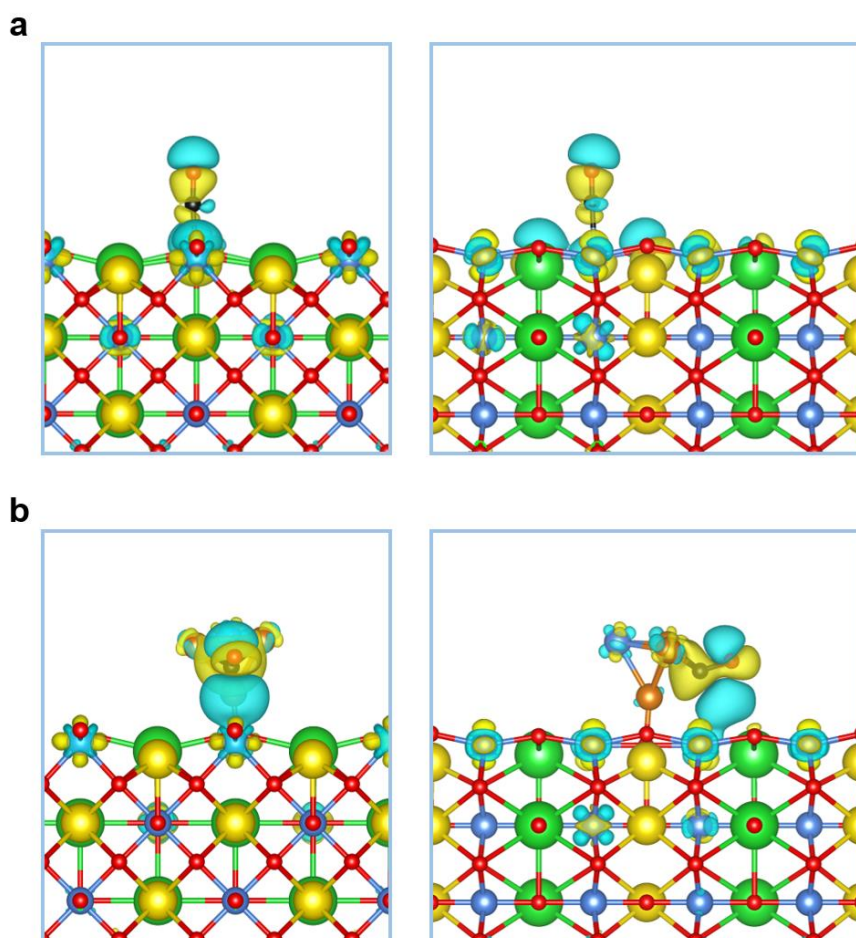
Figure S10. Charge density difference isosurfaces for CO* configuration over (a) PBF and (b) FeNi$_3$@PBF.

Figure S11. SEM image of the activated carbon used in this work.

2. Supporting table

Table S1. The correction of zero-point energy, enthalpy effect and entropy effect of the adsorbed and gaseous species.

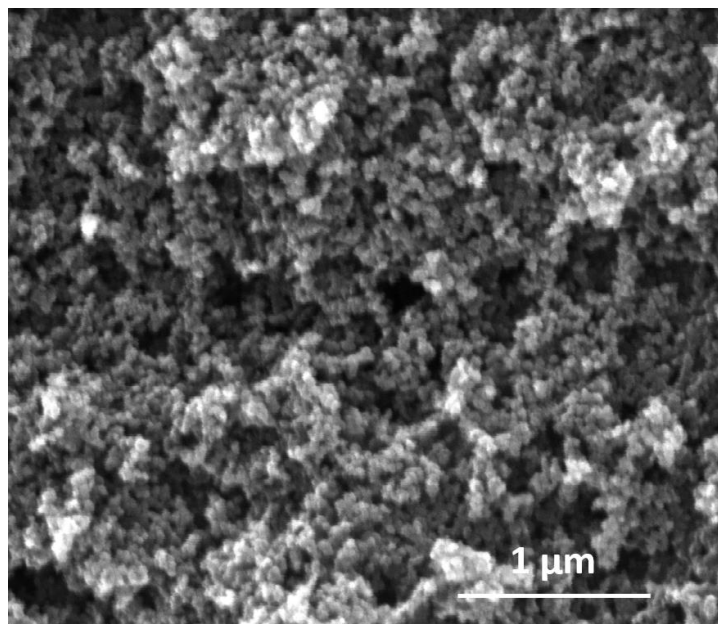|	ZPE (eV)	$\int C_p dT$ (eV)	TS (eV)
*CO_2	0.62	0.10	0.18
*CO	0.19	0.08	0.15
CO_2	0.31	0.10	0.65

Table S2. XPS analysis of O 1s for PBFNN and FeNi$_3$@PBFNN samples.

Sample	O 1s (eV)		$O_{lat.}$ (at.%)	$O_{ads.}$ (at.%)
	$O_{lat.}$	$O_{ads.}$		
PBFNN	528.7	530.8/532.1	51.49	49.51
FeNi$_3$@PBFNN	529.1	530.9/532.4	47.81	52.19

Table S3. XPS analysis of Ni 2p for PBFNN and FeNi$_3$@PBFNN samples.

Sample	Ni 2$p_{3/2}$ (eV)		Ni^0 (at.%)	Ni^{2+} (at.%)
	Ni^0	Ni^{2+}		
PBFNN	-	854.8/856.0	0	100
Fe-Ni@PBFNN	852.7/857.4	854.9/855.7	44.19	55.81

Table S4. XPS analysis of Fe 2p for PBFNN and FeNi$_3$@PBFNN samples.

Sample	Fe 2$p_{3/2}$ (eV)			Fe^0 (at.%)	Fe^{2+} (at.%)	Fe^{3+} (at.%)
	Fe^0	Fe^{2+}	Fe^{3+}			
PBFNN	-	709.9	711.4	0	59.4	40.6
FeNi@PBFNN	707.9	710.2	711.9	2.6	50.7	46.7

3. Supporting reference

[1] X.L. Yue, A. Arenillas, J.T.S. Irvine, Faraday Discuss. 190 (2016) 269–289.

[2] C. Liu, J. Pu, X. Chen, Z. Ma, X. Ding, J. Zhou, S. Wang, Int. J. Hydrogen Energ. 45 (2020) 11784–11790.

[3] C.Q. Wang, Z. Lu, J.W. Li, Z.Q. Cao, B. Wei, H. Li, M.H. Shang, C.X. Su, Renewable Energy 158 (2020) 410–420.

[4] A. Kulkarni, S. Giddey, S.P.S. Badwal, J. Solid State Electrochem. 19 (2015) 325–335.

[5] W. Cai, J. Liu, F. Yu, Q. Zhou, Y. Zhang, X. Wang, M. Liu, M. Ni, Int. J. Hydrogen Energ. 42 (2017) 21167–21176.

[6] J. Liu, J.S. Qiao, H. Yuan, J. Feng, C. Sui, Z.H. Wang, W. Sun, K.N. Sun, Electrochim. Acta 232 (2017) 174–181.

[7] C. Jiang, J. Ma, A.D. Bonaccorso, J.T.S. Irvine, Energy Environ. Sci. 5 (2012) 6973–6980.

[8] F. Yu, Y. Zhang, L. Yu, W. Cai, L. Yuan, J. Liu, M. Liu, Int. J. Hydrogen Energ. 41 (2016) 9048–9058.

[9] W. Bian, W. Wu, C.J. Orme, H. Ding, M. Zhou, D. Ding, Adv. Funct. Mater. 30 (2020) 1910096.

[10] J.W. Li, B. Wei, C.Q. Wang, Z.Y. Zhou, Z. Lu, Int. J. Hydrogen Energ. 43 (2018) 12358–12367.

[11] Q. Qiu, M. Zhou, W. Cai, Q. Zhou, Y. Zhang, W. Wang, M. Liu, J. Liu, Biomass & Bioenergy 121 (2019) 56–63.

[12] M. Ma, J. Qiao, X. Yang, C. Xu, R. Ren, W. Sun, K. Sun, Z. Wang, A.C.S. Appl, Mater. Interfaces 12 (2020) 12938–12948.